Optical and Quantum Electronics **29** *(1997) 579–590*

Numerical study on space–time pulse compression

M. PIETRZYK
Institute of Fundamental Technological Research, Polish Academy of Sciences, Świętokrzyska 21, 00-049 Warsaw, Poland

Received 21 June 1996; revised 22 January; accepted 23 January 1997

A numerical study of the properties of Gaussian pulses propagating in a planar waveguide under the combined effects of positive Kerr-type nonlinearity, diffraction in planar waveguides and anomalous or normal dispersion, is presented. It is demonstrated how the relative strength of dispersion and diffraction, the strength of nonlinearity and the initial spatial and temporal pulse chirps effect the parameters of pulse compression, such as the maximal compression factor and the distance to the point of maximal compression.

1. Introduction

The compression of optical pulses in Kerr-type nonlinear media have been subject to investigation for many years and continue to attract some attention [1, 2]. In single-mode fibres with anomalous group-velocity dispersion (GVD) and positive nonlinearity the pulse compression is based on the mechanism of higher-order soliton generation [3]. In single-mode fibres with normal GVD the pulse compression can be obtained in the configuration with a grating pair [4, 5]. In both cases self-phase modulation (SPM) induced by an intense pulse is used. However, the intense pump pulse propagating together with a weak probe pulse can also cause pulse compression by the mechanisms of so-called cross-phase modulation (XPM) [6], or induced-phase modulation (IPM) [7].

The possibility of pulse compression in non-dispersive nonlinear bulk media due to another nonlinear effect, that of self-focusing, is discussed in [8–10] with the aid of the paraxial ray approximation [8, 10], and by means of variational analysis [9]. Still another pulse compression technique that uses the self-confinement of two-dimensional spatial bright solitons propagating in non-dispersive bulk media is mentioned in [11], where a two-beam interference technique is used in order to ensure that a filamentation (a splitting of the beam into many sub-beams) does not occur.

Moreover, a simultaneous space–time collapse, which can occur in bulk media and in planar waveguides under the combined effect of nonlinearity, diffraction and anomalous dispersion, may also be useful for pulse compression [12, 13]. This kind of collapse gives rise to short pulses with an extremely high optical field [14–16]. It is realizable both in the case when dispersion and diffraction have comparable effects on pulse propagation and in the more general case when one of the above effects dominates (see [17]).

0306–8919

On the other hand, the interplay of normal dispersion and positive nonlinearity causes quite a different behaviour of the pulse. In optical fibres where diffraction terms are not included it leads to a monotonic pulse spreading. However, the inclusion of the diffraction term, which is necessary for a planar waveguide, can lead to a pulse compression, as was described in [17, 18]. In addition, in a planar waveguide, normal dispersion slows the self-focusing of the pulse and causes a splitting of the pulse into two pulses [18, 36]. The effect of pulse splitting was also observed in the bulk media [12].

In this paper the compression of a pulse propagating in a planar, self-focusing nonlinear planar waveguide in the regime of anomalous and normal dispersion is considered. The structure of the paper is as follows. In Section 2 the nonlinear Schrödinger equation describing dispersive pulse propagation in nonlinear planar waveguides and the parameters of pulse compression are introduced. In Section 3 an estimation of the condition of pulse collapse is made with the aid of the so-called method of moments [19]. Numerical results describing the influence of the magnitude of nonlinearity, the relative strength of dispersion and diffraction and the spatial and temporal chirp of the initial Gaussian pulse on the pulse compression parameters are discussed in Section 4.

2. Basic equations

It is well known that starting from the Maxwell equations for the envelope $U(x, y, z, t)$ of the electric field

$$E(x, y, z, t) = U(x, y, z, t)\mathrm{e}^{-\mathrm{i}(\omega t - n_0\beta_0 z)}$$

propagating along the z-axis in a planar waveguide with positive, instantaneous Kerr-type nonlinearity, one obtains the two-dimensional nonlinear Schrödinger equation (NSE) [18]:

$$\mathrm{i}\frac{\partial}{\partial\zeta}U - \frac{1}{2}\sigma\frac{\partial^2}{\partial\tau^2}U + \frac{1}{2}\frac{\partial^2}{\partial\xi^2}U + N^2|U|^2U = 0 \tag{1}$$

if the paraxial and the slowly varying envelope approximations are applied and the term $\nabla \cdot (\nabla E)$, the shock term [20] proportional to $\partial(|E|^2E)/\partial t$ and higher-order dispersion effects can be neglected.

In Equation 1, $\zeta = z/z_f$ is the normalized longitudinal spatial coordinate, $\xi = x/w_0$ is the normalized transverse spatial coordinate, $\tau = (t - \beta_1 z)/t_0$ is the normalized local time, $\sigma = \beta_2 z_f/t_0^2$ represents the relative strength of dispersion and diffraction, $N = \beta_0 U_0 w_0\sqrt{n_0 n_2}$ parameterizes the strength of nonlinearity, $\beta_0 = \omega/c$ is a wave number, $\beta_n = \mathrm{d}^n\beta/\mathrm{d}\omega^n$ are dispersion terms, $z_f = \beta_0 n_0 w_0^2$ is the Fresnel diffraction length, w_0 is the spatial width of the input pulse, t_0 is the temporal width of the input pulse (i.e., duration of the input pulse), U_0 is the peak amplitude of the input pulse, and $n = n_0 + n_2|U|^2$ is the refraction index for the Kerr-type nonlinear media. Recall that $\sigma > 0$ corresponds to the normal dispersion and $\sigma < 0$ corresponds to the anomalous dispersion.

As the initial condition the Gaussian chirped pulse is taken. This is given by (*cf*. [21])

$$U(\xi, \tau, \zeta = 0) = \mathrm{e}^{-\xi^2(1+\mathrm{i}C_\xi)/2}\mathrm{e}^{-\tau^2(1+\mathrm{i}C_\tau)/2} \tag{2}$$

where C_ξ (C_τ) is the spatial (temporal) pulse chirp (the focusing spatial chirp corresponds to $C_\xi < 0$ and the focusing temporal chirp corresponds to $\mathrm{sgn}(-\sigma C_\tau) < 0$).

Here a pulse is characterized by its spatial width, $w_\xi(\zeta)$, and temporal width, $w_\tau(\zeta)$, which are defined by

$$U(w_\xi, 0, \zeta) = \frac{1}{e} U(0, 0, \zeta) \quad \text{and} \quad U(0, w_\tau, \zeta) = \frac{1}{e} U(0, 0, \zeta)$$

The maximal compression factor is also introduced:

$$c_{\max} = \frac{\tau_0}{w_{\tau\,\min}(\zeta_m)}$$

where $w_{\tau\,\min}(\zeta_m)$ is the minimal temporal width of the pulse (see [18, 22]). In the following ζ_m is called the position of the minimal pulse width.

The solution of NSE (Equation 1) with the initial condition given by Equation 2 can describe a propagation of a dispersive Gaussian pulse in nonlinear planar waveguides. It is worth remarking that for the anomalous dispersion regime a solution of this equation can also describe a dispersionless elliptic Gaussian beam [23, 24] (i.e. a CW beam with an elliptic Gaussian transverse profile) propagating in a nonlinear bulk media.

In this paper the case of $\sigma = -1$ is referred to as the cylindrically symmetric spatiotemporal pulse; the case of $\sigma \neq -1$ is to be referred to as the asymmetric spatiotemporal pulse.

In the particular case of the cylindrical spatiotemporal pulse a simple analytic solution of the NSE exists which describes the behaviour of a beam propagating in nonlinear media by means of variational approximation [14] or by means of the scaled complex rays formulation within the so-called ABCD matrix formalism (see [25, 26]). For the asymmetric spatiotemporal pulse only the semi-analytical approach of [23, 24] is known in the literature.

It is known that some solutions of the two- or three-dimensional NSE can develop into a singularity of the electric field when the initial pulse power exceeds a certain critical value [14]. This phenomenon, known as a pulse collapse, can occur simultaneously in space and time for a pulse propagating in a planar waveguide with anomalous GVD [14, 15], and also for a dispersionless beam propagating in a self-focusing bulk medium. This singularity, however, is obviously non-physical, for it emerges just as an artefact of the paraxial approximation made when deriving the NSE. In order to avoid this limitation, either a non-paraxial treatment of the process of self-focusing [27] or some other effects, such as the nonlinear absorption and the saturation of the nonlinear refractive index, should be taken into consideration. On the other hand, the appearance of a non-physical singularity in numerical simulations based on the NSE can serve as an indication of a real collapse taking place in a certain point of space. This is in fact the criterion used in Section 4.

The study of the details of the development of the pulse collapse is left beyond the scope of this paper. Instead, the task here is to determine the values of the parameters σ and N^2 for which the pulse collapse can occur. For this the so-called method of moments [28] could be used. However, it gives only an estimation of the sufficient conditions of the pulse collapse, whereas the collapse can in fact occur at an earlier time or a shorter propagation distance [10]. More precise conditions will be obtained by the numerical simulations presented in Section 3 (*cf.* also [14]).

3. Sufficient conditions of pulse collapse

The method of moments originates from the paper of Vlasov *et al.* [28]. It can be used as an approach to the determination of whether a given initial wave pulse can collapse to a singular point in a finite period of time [29]. An application of the method of moments to the NSE may be found in [19].

In order to formulate the condition of collapse in terms of the strength of nonlinearity, N^2, and the relative strengths of dispersion and diffraction, σ, the second moment of intensity is first introduced:

$$I(\zeta) = \int_{-\infty}^{\infty}\int_{-\infty}^{\infty} (\xi^2 + \bar{\tau}^2)|U|^2 \, \mathrm{d}\xi \, \mathrm{d}\bar{\tau}$$

where U is a solution of the NSE given by Equation 1, with the normalization $\bar{\tau} = (-\sigma)^{-1/2}\tau, (\sigma \neq 0)$.

Parameter I can be interpreted as the effective beam size, measuring the size of the area to which most of the energy is confined.

Assuming that U decays suitably as $r \to \infty$, one can obtain [19]

$$\frac{\mathrm{d}^2 I}{\mathrm{d}\zeta^2} = \ddot{I} = 4E \tag{3}$$

where E is the Hamiltonian of the NSE

$$E = \iint \left(\frac{1}{2}\left|\frac{\partial U(\xi,\bar{\tau})}{\partial \xi}\right|^2 + \frac{1}{2}\left|\frac{\partial U(\xi,\bar{\tau})}{\partial \bar{\tau}}\right|^2 - \frac{1}{2}N^2|U(\xi,\bar{\tau})|^4 \right) \mathrm{d}\xi \, \mathrm{d}\bar{\tau}$$

Because E remains constant during a pulse propagation, i.e. it is independent of ζ, Equation 3 may be integrated twice to give:

$$I(\zeta) = 2E\zeta^2 + \dot{I}(0)\zeta + I(0)$$

where $\dot{I} = \mathrm{d}I/\mathrm{d}\zeta$.

If the right-hand side of the above equation vanished, then the pulse width (both spatial and temporal) will decrease to zero in a finite distance leading to beam collapse. Therefore a sufficient condition for collapse can occur if the following conditions are satisfied [19, 21, 29]:

$$\begin{aligned} &E < 0 \\ &E = 0 \quad \text{and} \quad \dot{I}(0) < 0 \\ &E > 0 \quad \text{and} \quad \dot{I}(0) < -\sqrt{8EI(0)} \end{aligned} \tag{4}$$

For a Gaussian input pulse, given by Equation 2, Hamiltonian E can be expressed in the following form

$$E = \frac{1}{2}\iint \left[\left(\xi^2 - \sigma^2\bar{\tau}^2\right)\mathrm{e}^{-\xi^2}\mathrm{e}^{-\sigma\bar{\tau}^2} - N^2\mathrm{e}^{-2\xi^2}\mathrm{e}^{-2\sigma\bar{\tau}^2} \right] \mathrm{d}\xi \, \mathrm{d}\bar{\tau} = \frac{1}{4}\sqrt{-\sigma}\pi(1 - \sigma - N^2)$$

In the particular case of flat phase front, $C_\xi = C_\tau = 0$, we obtain that $\dot{I}(0) = 0$ and because of this the last two criteria in Equation 4 are not satisfied. The first criterion, $E < 0$, yields

$$N^2 > 1 - \sigma \tag{5}$$

Equation 5 may be considered as the sufficient condition of the pulse collapse in terms of the strength of nonlinearity, N^2, which is proportional to the peak amplitude, $|U_0|^2$, and the relative strength of dispersion and diffraction, σ. The magnitude of the parameter N^2

which is sufficient for the pulse collapse to occur increases linearly with $|\sigma|$. This is not unexpected because the collapse of the pulse occurs when the self-focusing caused by the nonlinearity dominates over the broadening of a pulse, which is due to the diffraction and dispersion. It is obvious that the smaller the values of the parameter $|\sigma|$ are, the weaker is the influence of the dispersion on the pulse broadening.

Note that the sufficient conditions of pulse collapse can be formulated also in terms of the critical initial power, P_c, of the pulse as follows [21, 24]

$$\frac{P_c}{P_0} = \left[\sqrt{|\sigma|} + \frac{1}{\sqrt{|\sigma|}}\right] \geq 1$$

where $P_c(\sigma) = \int |U|^2 \,d\tau \,d\xi = \pi |U_0|^2 \left(1/\sqrt{|\sigma|}\right), P_0 = 2\pi$ is the initial power of the cylindrically symmetric pulse (i.e. $\sigma = 1$).

We conclude that the decrease of the parameter $|\sigma|$ leads to the decrease of the critical amplitude, $|U_0|^2$, and to the increase of the critical power, P_c.

Note, that the collapse criteria obtained with the aid of the method of moments for the particular case of the spatiotemporal symmetric pulse agrees with the result of the variational approximation in [10, 14].

4. Numerical results and discussion

In this section, the results of the numerical solution of the $(2+1)$-dimensional NSE by means of the well-known split-step spectral method (SSSM) [30] with the two-dimensional (2d) fast Fourier transform [31] are presented. The calculations were performed on a two-dimensional grid with 512×512 points (transverse steps, $\Delta\xi = \Delta\tau = 0.08$) and with a longitudinal step depending on the nonlinearity so that for $N^2 = 1, \Delta\zeta = 0.01$. Because of the lack of spatial–temporal cylindrical symmetry of the problem it is not possible to simplify calculations by reducing the two-dimensional fast Fourier transform to the one-dimensional Hankel transform developed in [32, 33]. Several checks of our numerical procedure were made, including a simulation of beam propagation in the absence of group-velocity dispersion ($\sigma = 0$), repeated testing with different transverse grid and longitudinal step lengths, and the monitoring of pulse energy during each simulation. The latter was kept constant with a relative error of less than 0.000 05.

As an initial condition in the numerical calculations the Gaussian pulse given by Equation 2 was taken. First, for the case of the anomalous dispersion regime the conditions of pulse collapse predicted by the method of moments is compared with those obtained from numerical calculations. Further, with the aid of numerical calculations, the influence is studied of the strength of nonlinearity, relative strength of dispersion and diffraction and spatial and temporal pulse chirps on pulse compression parameters. The above analysis is performed for both the anomalous and the normal dispersion regime.

4.1. The anomalous dispersion regime

In this section the influence of the parameters σ and N^2 on the pulse collapse and compression will be considered.

In Fig. 1, a comparison of the conditions of the collapse of pulse predicted by the method of moments with those obtained by numerical calculations is presented. In the numerical procedure the occurrence of pulse collapse was identified with the discontinuity of the phase $\phi(0, 0, \zeta)$ in the central point of the pulse $u = |u|e^{i\phi}$, and with non-monotonic

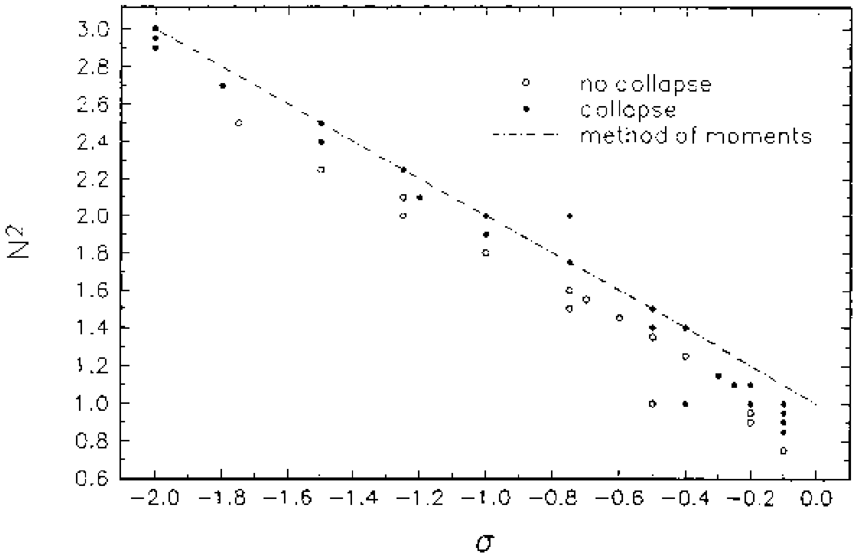

Figure 1 Comparison of the sufficient conditions for pulse collapse predicted by the method of moments (straight line) and numerical calculations (filled circle points denote pulse collapse and empty circle points indicate no collapse). This was performed for an initial Gaussian pulse with a flat phase front, propagating in a medium described by two parameters: the strength of the nonlinearity, N^2, and the relative strength of dispersion and diffraction, σ.

behaviour of the intensity in the central point of the pulse after the collapse point has been reached. The results of numerical simulations are plotted by two sets of points corresponding to the cases when, respectively, the pulse collapse occurs or does not occur. The prediction obtained by the method of moments is given by the straight line $N^2 = 1 - \sigma$ (see Equation 5). The boundary line between the collapse and the no-collapse regions, obtained from the numerical data is approximately described by $N^2 \approx (0.85 - \sigma)$. It is parallel to the straight line predicted by the method of moments, unless the absolute value of σ is too small.

Therefore, for both methods, the magnitude of the parameter N^2 which is sufficient for the pulse collapse to occur increase linearly with $|\sigma|$. The discrepancy appears to be due to the theoretical idealization of the picture of the collapse where all the energy of the pulse goes to the singularity point. This also explains why conditions of numerical collapse are typically softer than those predicted by the method of moments described in Section 3.

The study of details of pulse collapse is left beyond the task of this paper. Instead, a study is made of the influence of the relative strength of dispersion and diffraction, the nonlinearity and the spatial and temporal chirps on the parameters of pulse compression under the condition that pulse collapse does not occur.

Figures 2 and 3 represent the results of calculations of the influence of the relative strength of dispersion and diffraction, σ, on the maximal compression factor, c_{max}, and on the position of the minimal pulse width, ζ_{m}, for different values of the strength of nonlinearity, N^2 and for a Gaussian initial pulse with a flat phase front. As could be expected, the parameters of pulse compression, c_{max} and ζ_{m}, increase monotonically with the increase of N^2 and the decrease of σ until collapse conditions are reached. This behaviour is

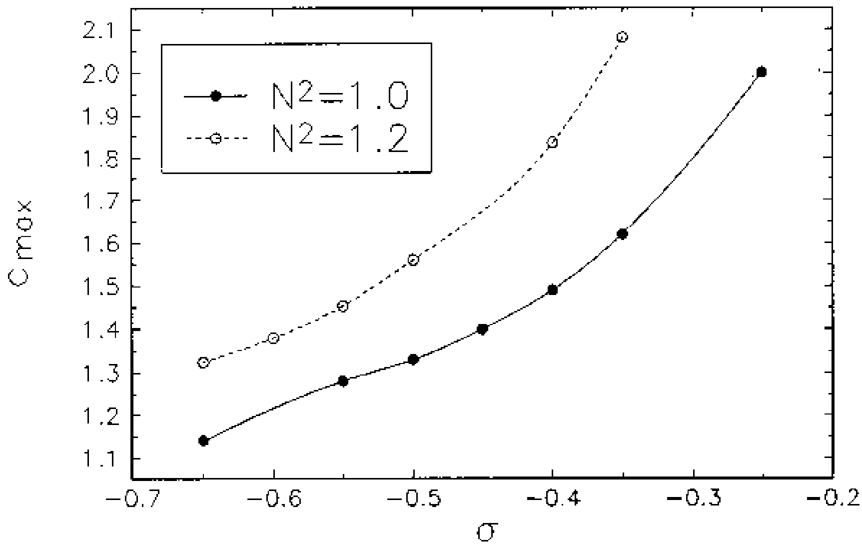

Figure 2 The maximum compression ratio, c_{max}, as a function of the relative strength of dispersion and diffraction, $\sigma < 0$, for a different value of the strength of nonlinearity, N^2, and for an initial Gaussian pulse with a flat phase front.

obvious from the fact that increase of N^2 causes increase of pulse self-focusing, it helps to concentrate pulse energy in the centre. In addition, a decrease of σ causes a decrease of dispersion broadening of the pulse.

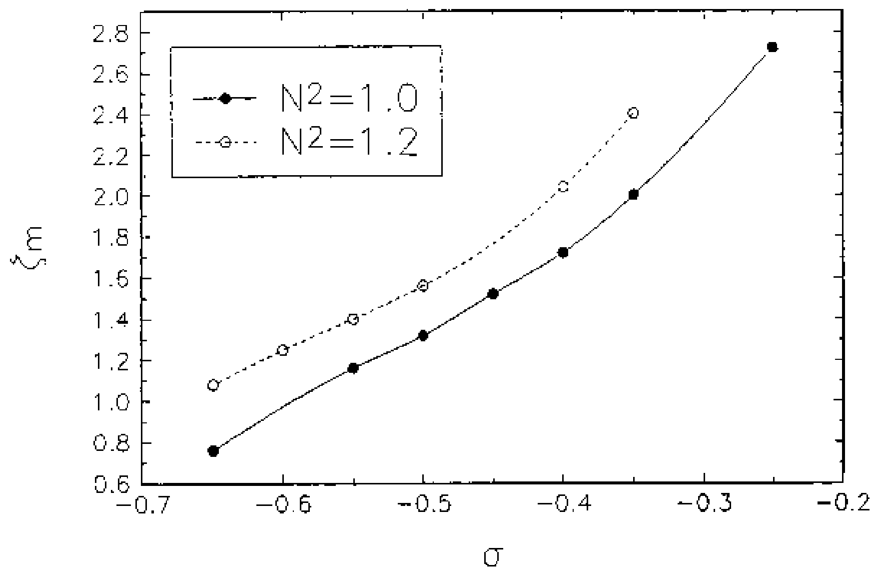

Figure 3 The distance to the point of minimal pulse width, ζ_m, as a function of the relative strength of dispersion and diffraction, $\sigma < 0$, for a different value of the strength of nonlinearity, N^2, and for an initial Gaussian pulse with a flat phase front.

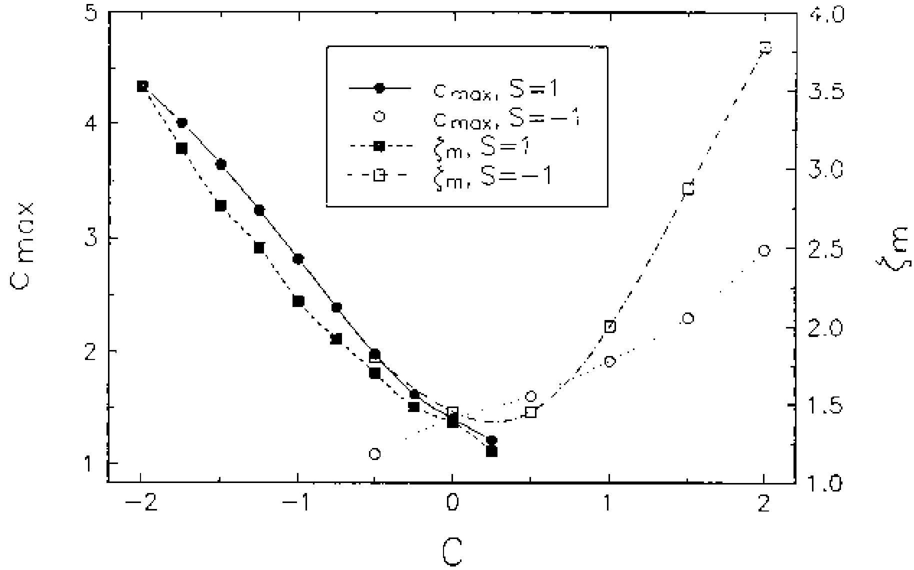

Figure 4 The maximal compression factor, c_{max}, and the distance to the point of the minimal pulse width, ζ_m, as a function of the initial spatial and temporal pulse chirps, $C_\xi = C$ and $C_\tau = \pm C$, respectively. Spatial focusing chirp occurs for $C < 0$, temporal focusing chirp occurs for $C_\tau < 0$, $\sigma = -0.5$ and $N^2 = 1.0$.

In Fig. 4 the results of numerical simulations of the influence of the initial spatial, $C_\xi = C$, and two cases of temporal, $C_\tau = \pm C$, chirps on the pulse compression parameters are presented. In order to distinguish between the above two cases we introduce a parameter

$$S = \mathrm{sgn}(-C_\xi C_\tau \sigma)$$

which equals 1 for the case of focusing (defocusing) temporal and spatial chirps and equals -1 for the case of focusing (defocusing) temporal and defocusing (focusing) spatial chirps.

As could be expected, the focusing spatial and temporal chirps, $C < 0, S = 1$, cause the increase of the pulse compression parameters. The explanation is that a defocusing chirp spreads the energy out from the centre of the pulse, whereas a focusing chirp concentrates it there. As a result, the nonlinearity-induced phase curvature of the field is, respectively, reduced or enhanced. A similar effect of the focusing chirp of the initial pulse takes place in the region close to the collapse. Namely, the focusing spatial chirp can hasten the collapse, whereas a defocusing chirp can either delay or eliminate it entirely [17].

More interesting is the case of $S = -1$ (i.e. the spatial focusing chirp and the temporal defocusing chirp occur simultaneously). The increase of the maximal compression factor occurs only for the case of the focusing temporal chirp, $C > 0$, whereas this is not always true for a spatial focusing chirp $C < 0$, see Fig. 4. One can conclude that the temporal chirp has a larger effect on the temporal pulse compression than the spatial one. One can expect the reverse situation in the case of spatial compression of the pulse.

4.2. Normal dispersion regime

In the case of a normal dispersion regime the collapse of the pulse does not occur. However, owing to the spatiotemporal coupling occurring in the nonlinear medium when both the diffraction and the dispersion effects take place a pulse compression can be obtained [18].

In this section a study is made of the influence of the relative strength of dispersion and diffraction, the nonlinearity and the spatial and temporal pulse chirps on the parameters of pulse compression.

It is seen from Fig. 5 that the maximal compression factor, $c_{\max}$, monotonically decreases with σ, and increases with N^2. It is clear because a smaller value of the parameter σ has a weaker influence on the dispersion broadening of the pulse, moreover the increase of N^2 leads to the increase of the spatiotemporal coupling and nonlinearity-induced phase curvature of the field. Ultimately both effects lead to the temporal compression of the pulse.

From Fig. 6 it is seen that for sufficiently small values of σ the parameter ζ_{m} decreases with N^2. However it appears to be practically independent on σ once a certain threshold level of N^2 is reached. This fact was explained in [17] by means of the periodic beam narrowing of higher-order spatial solitons. A different behaviour takes place at larger values of σ ($\sigma > 0.25$). Namely, at first ζ_{m} increases with N^2 for sufficiently small N^2 and then it slowly decreases after reaching a maximal value at the certain value of N^2. This behaviour can be explained by the fact that at small nonlinearities the effects of dispersion prevent a creation of spatial solitons.

In Fig. 7 the results of numerical calculations of the influence of the initial pulse chirp on the parameters of pulse compression c_{m} and ζ_{m} are presented. The focusing spatial and temporal chirps, $C < 0, S = 1$, cause the increase of the compression parameters ($c_{\max}$ and $\zeta_{\max}$) and this behaviour appears to be similar to that which we have previously observed in Fig. 4 for the anomalous dispersion regime. However, in the case of the anomalous GVD, $c_{\max}$ grows with C much faster that in the case of normal GVD. Namely, for the

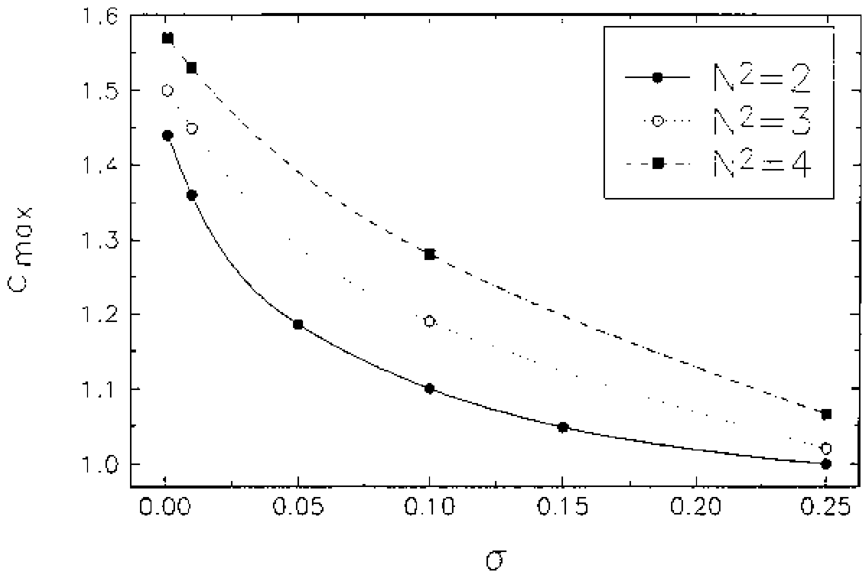

Figure 5 The maximal compression factor, c_{max}, as a function of the relative strength of dispersion and diffraction, $\sigma > 0$, for a different value of the strength of nonlinearity, N^2, and for an initial Gaussian pulse with a flat phase front.

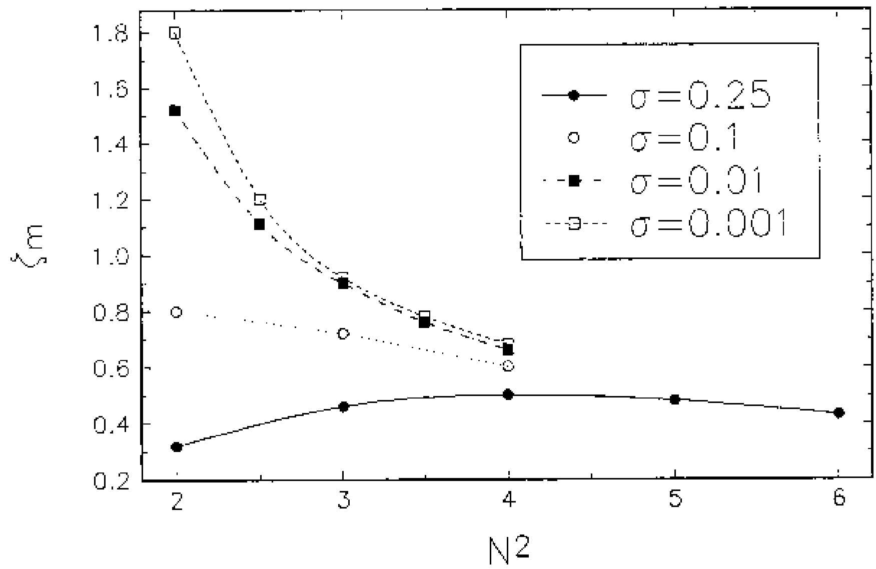

Figure 6 The distance to the point of the minimal pulse width, ζ_m, as a function of the strength of nonlinearity, N^2, for a different value of the relative strength of dispersion and diffraction, $\sigma > 0$, and for an initial Gaussian pulse with a flat phase front.

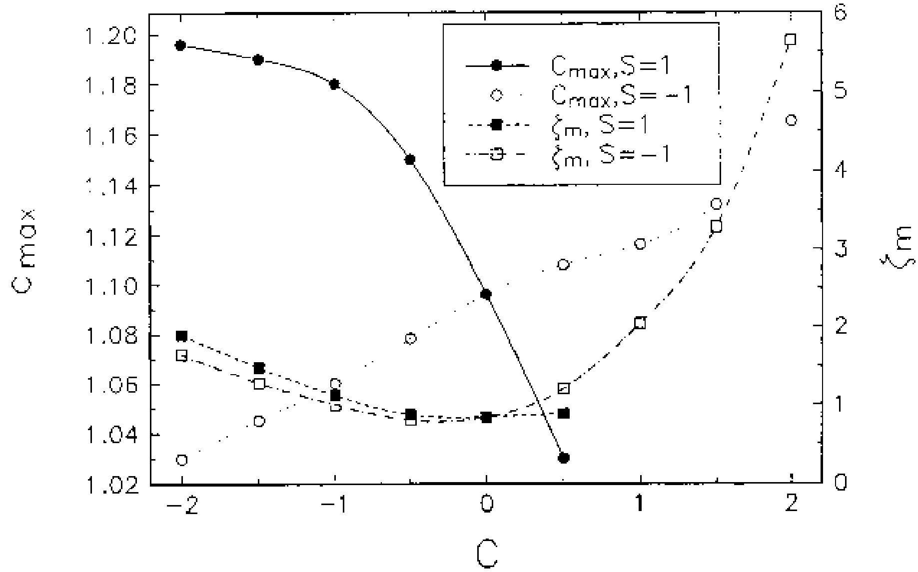

Figure 7 The maximal compression factor, c_{max}, and the distance to the point of the minimal pulse width, ζ_m, as a function of the initial spatial and temporal pulse chirps, $C_\xi = C$ and $C_\tau = \pm C$, respectively. Spatial focusing chirp occurs for $C_\xi < 0$, temporal focusing chirp occurs for $C_\tau > 0, \sigma = 0.1$ and $N^2 = 2.0$.

anomalous GVD the maximal compression factor for a chirped initial pulse with $C = -2$ is three times larger than that for an initial pulse with a flat phase front ($C = 0$, i.e. $c_{\max}(C = -2) = 3 \times c_{\max}(C = 0)$. For the normal GVD the increase of $c_{\max}$ is rather slow, e.g. $c_{\max}(C = -2) = 1.1 \times c_{\max}(C = 0)$, and a saturation of the maximal compression factor occurs for the initial chirps below −2 (see Fig. 7).

Moreover, for the case of $C < 0, S = -1$ (i.e. the spatial focusing chirp and the temporal defocusing chirp) the maximal compression factor increases only for the focusing temporal chirp, whereas this is not always true for a spatial focusing chirp $C_\xi < 0$.

5. Conclusions

In this paper, the physical conditions of collapse and compression of dispersive Gaussian pulses propagating in waveguide with positive Kerr-type nonlinearity, diffraction and anomalous or normal dispersion were investigated.

The values of the relative strength of dispersion and diffraction, σ, and the strength of nonlinearity, N^2, for which the pulse collapse can occur were determined. For this purpose an estimation was first given by the method of moments [28]. More precise conditions were obtained by means of the numerical simulations based on the $(2+1)$-dimensional nonlinear Schrödinger equation (see Section 4).

A pulse compression was characterized by two parameters: the maximal compression factor, $c_{\max}$, and the distance to the point of the maximal compression, ζ_{m}, (see Section 2). By means of a numerical simulation, how these two parameters depend on the parameters N^2 and σ, and the initial spatial and temporal pulse chirps was studied. It was demonstrated that in the regime of both anomalous and normal dispersion the increase of the nonlinearity and the decrease of the relative strength of dispersion and diffraction cause an increase of the maximal compression factor. Moreover, in the case of the anomalous dispersion regime the compression factor is maximal in the region $(1 - \sigma) \lesssim N^2$.

Furthermore, it was observed that the increase of the focusing temporal and spatial chirps of the initial pulse lead to an increase of the maximal compression factor, $c_{\max}$. In the case of the anomalous GVD, $c_{\max}$ grows with chirp, C, much faster than in the case of normal GVD, for which a saturation of the maximal compression factor occurs.

Moreover, the increase of the focusing temporal chirp might lead, even in the presence of the defocusing spatial chirp, to an increase of the maximal compression factor, $c_{\max}$, whereas the defocusing temporal chirp always leads to a decrease of $c_{\max}$, even in the case of the focusing spatial chirp. It may be concluded, therefore, that the temporal chirp has a larger effect on the maximal pulse compression factor than has the spatial chirp. Conversely, it is expected that the spatial focusing chirp has a larger impact on the beam than the temporal chirp, independently of its sign.

Acknowledgement

The author wishes to thank Docent W. Nasalski for the suggestion of this topic and his remarks.

References

1. K. TAMURA and M. NAKAZAWA, *Opt. Lett.* **21** (1996) 68.
2. K. C. CHAN and H. F. LIU, *IEEE J. Quantum Electron.* **31** (1995) 2226.
3. K. C. CHAN and H. F. LIU, *Opt. Lett.* **19** (1994) 49.
4. R. F. X. A. M. MOLS and G. J. ERNST, *Opt. Comm.* **94** (1992) 509.
5. A. M. WEINER, J. P. HERITAGE and R. H. STOLEN, *J. Opt. Soc. Am. B* **5** (1988) 364.

6. G. P. AGRAWAL, P. L. BALDECK and R. R. ALFANO, *Opt. Lett.* **14** (1989) 137.
7. M. JAMASHITA and K. TORIZUKA, *Jap. J. of Appl. Phys.* **29** (1990) 294.
8. J. T. MANASSAH, P. L. BALDECK and R. R. ALFANO, *Opt. Lett.* **13** (1988) 1090.
9. M. KARLSSON, D. ANDERSON, M. DESAIX and M. LISAK, *Opt. Lett.* **16** (1991) 1373.
10. J. T. MANASSAH and B. GROSS, *Opt. Lett.* **17** (1992) 976.
11. D. H. REITZE, A. M. WEINER and D. E. LEAIRD, *Opt. Lett.* **16** (1991) 1409.
12. P. CHERNEV, and V. PETROV, *Opt. Lett.* **17** (1992) 172.
13. S. K. TURISYN, *Phys. Rev. A* **47** (1992) 27.
14. M. DESAIX, D. ANDERSON and M. LISAK, *J. Opt. Soc. Am. B* **8** (1991) 2082.
15. Y. SILBERGER, *Opt. Lett.* **15** (1990) 1282.
16. J. T. MANASSAH, *Opt. Lett.* **16** (1991) 563.
17. A. T. RYAN and G. P. AGRAWAL, *J. Opt. Soc. Am. B* **12** (1995) 2382.
18. A. T. RYAN and G. P. AGRAWAL, *Opt. Lett.* **20** (1995) 306.
19. F. H. BERKSHIRE and J. D. GIBBON, *Stud. Appl. Math.* **69** (1983) 229.
20. J. E. ROTHENBERG, *Opt. Lett.* **17** (1992) 583.
21. X. D. CAO, G. P. AGRAWAL and C. J. McKINSTRIE, *Phys. Rev. A* **49** (1994) 4085.
22. R. F. X. A. M. MOLS and G. J. ERNST, *Opt. Comm.* **94** (1992) 509.
23. V. MAGNI, G. CERULLO, S. DE SILVESTRI and A. MONGUZZI, *J. Opt. Soc. Am. B* **12** (1995) 476.
24. F. CORNOLTI, M. LUCCHESI and B. ZAMBON, *Opt. Comm.* **75** (1990) 129.
25. W. NASALSKI, *Opt. Appl.* **XXIV** (1994) 4.
26. W. NASALSKI, *Opt. Comm.* **119** (1995) 218.
27. M. D. FEIT and J. A. FLECK, JR, *J. Opt. Soc. Am. B* **5** (1988) 633.
28. S. N. VLASOV, V. A. PETRISHCHEV and V. I. TALANOV, *Izv. Vuz Radiofiz* **14** (1971) 1353.
29. J. J. RASMUSSEN and K. RYPDAL, *Phys. Scripta* **33** (1986) 481.
30. G. P. AGRAWAL, *Nonlinear Fiber Optics* (Academic Press, Boston, 1989).
31. W. H. PRESS, S. A. TEUKOLSKY, W. T. VETTERLING and B. P. FLANNERY, *Numerical Recipes in Fortran* (Cambridge University Press, 1992).
32. A. E. SIEGMAN, *Opt. Lett.* **1** (1977) 13.
33. M. VAN VELDHUIZEN, R. NIEUWENHUIZEN and W. ZIJL, *J. of Comp. Phys.* **110** (1994) 196.
34. G. FIBICH, V. M. MALKIN and G. C. PAPANICOLAOU, *Phys. Rev. A*. **52** (1995) 4218.
35. V. VYSLOUKH and T. MATVEEVA, *Bull. Russ. Acad. Sci. Phys.* **56** (1992) 1289.
36. D. BURAK and R. BINDER, *Proc. Quantum Electron. and Laser Science Conf.*, Anaheim, CA (1996) QPD 12.